Available online at www.sciencedirect.com
ScienceDirect
Trans. Nonferrous Met. Soc. China 35(2025) 4242−4252
Transactions of Nonferrous Metals Society of China
www.tnmsc.cn

Selective depression effect of sodium fluosilicate in flotation separation of cassiterite and dravite

Yang NI[1], Wen-juan SUN[1], Hai-sheng HAN[1,2,3], Wei SUN[1,2], Jun-hao FU[1], Yong-biao CHENG[1]

1. School of Minerals Processing and Bioengineering, Central South University, Changsha 410083, China;
2. Engineering Research Center of Ministry of Education for Carbon Emission Reduction in Metal Resource Exploitation and Utilization, Central South University, Changsha 410083, China;
3. Technology Research Center of Hunan Province for Comprehensive Utilization of Associated Fluorite and Fluorine Chemical Engineering, Chenzhou 423000, China

Received 22 April 2024; accepted 11 December 2024

Abstract: The flotation separation of cassiterite and dravite was realized using lead complexes of benzohydroxamic acid (Pb-BHA) as a collector and sodium fluosilicate (SF) as a depressant. Zeta potential tests confirmed that SF enabled the selective depression of dravite. The results of Fourier transform infrared (FTIR) spectroscopy analysis demonstrated that hydroxyl-containing groups in the hydrolysis products of SF selectively chemisorbed on the surface of dravite. X-ray photoelectron spectroscopy (XPS) analysis results further demonstrated the strong chemisorption of SF hydrolysis products (F-containing groups and hydroxyl-containing groups) on dravite (Mg sites). Consequently, the adsorption of Pb-BHA on dravite was selectively prevented. Based on the results, a selective depression model of SF on cassiterite and dravite was proposed.

Key words: selective depression effect; flotation separation; sodium fluorosilicate; cassiterite; dravite; benzohydroxamic acid

1 Introduction

Tin, with its low melting point, stability, ductility, non-toxicity, and corrosion resistance, is essential in both production and daily life [1]. In contemporary industrial practice, cassiterite remains the predominant raw material for the extraction of tin metal. However, with the exploitation of tin resources, the easily separable high-grade deposits are diminishing. This trend is prompting a shift towards the development and utilization of tin resources characterized by fine particle sizes, low grades, and complex mineral compositions [2,3]. Under these circumstances, froth flotation technology, which is more suitable for the separation of fine-grained minerals [4−8], is increasingly becoming the main method for the recovery of such tin resources, replacing the traditional heavy separation [9].

With the intensive study of cassiterite flotation technology, many collector systems have been developed. Among these, the benzohydroxamic acid system is the most representative collector system [10]. Using benzohydroxamic acid as a collector, combined with various activators (Pb^{2+}, Zn^{2+}, etc.) and depressants (sodium carboxymethyl cellulose, sodium hexametaphosphate, etc.), it is possible to achieve the flotation separation of cassiterite from common gangue minerals like calcite

Corresponding author: Hai-sheng HAN, Tel: +86-731-88830482, E-mail: hanhai5086@csu.edu.cn;
Yong-biao CHENG, Tel: +86-18104588418, E-mail: cyb8575@126.com
https://doi.org/10.1016/S1003-6326(25)66941-X

and quartz [11−15]. In addition, other hydroxamic acid-based collectors present favorable collecting ability in the flotation separation of cassiterite. Salicylhydroxamic acid exhibits superior selectivity and collecting ability for cassiterite compared to benzohydroxamic acid [16]. The utilization of cinnamon hydroxamic acid combined with Pb^{2+} enables the flotation separation of cassiterite from calcite [17]. In terms of reagent optimization, previous researchers designed and synthesized a series of N-phenylalkanoyl hydroxamic acids (NPHAs). In particular, the collecting ability of NPHA-6 and NPHA-8 was found to be superior to that of benzohydroxamic acid in the absence of activators and frothers [18]. Furthermore, the metal-organic coordination technique has been found to significantly improve the collecting ability and selectivity of the collector for cassiterite [19,20].

In prior cassiterite flotation studies, gangue minerals such as calcite and quartz were the main subjects. Currently, certain gangue minerals, such as tourmaline [21], have been found to significantly affect the recovery of tin resources. However, the flotation research on these gangue minerals remains largely insufficient. Therefore, in this work, we focused on dravite (a typical tourmaline [22]) and cassiterite, solving the problem of flotation separation of these two minerals with the aim of offering a theoretical foundation and technical reference for the development of dravite-associated refractory tin resources.

2 Experimental

2.1 Materials

Block-shaped crystals of cassiterite and dravite were obtained from Sichuan Province and Yunnan Province, China, respectively. The high purities of cassiterite and dravite were confirmed by X-ray diffraction (XRD) patterns, as shown in Fig. 1. Firstly, block-shaped crystals of dravite and cassiterite were crushed and ground successively. Subsequently, wet sieving was used to obtain products of two size fractions: 0.0385−0.074 mm; <0.0385 mm. The products of 0.0385−0.074 mm were used for micro-flotation experiments. The products of <0.0385 mm were further ground to serve as raw materials for zeta potential, FTIR, and XPS tests.

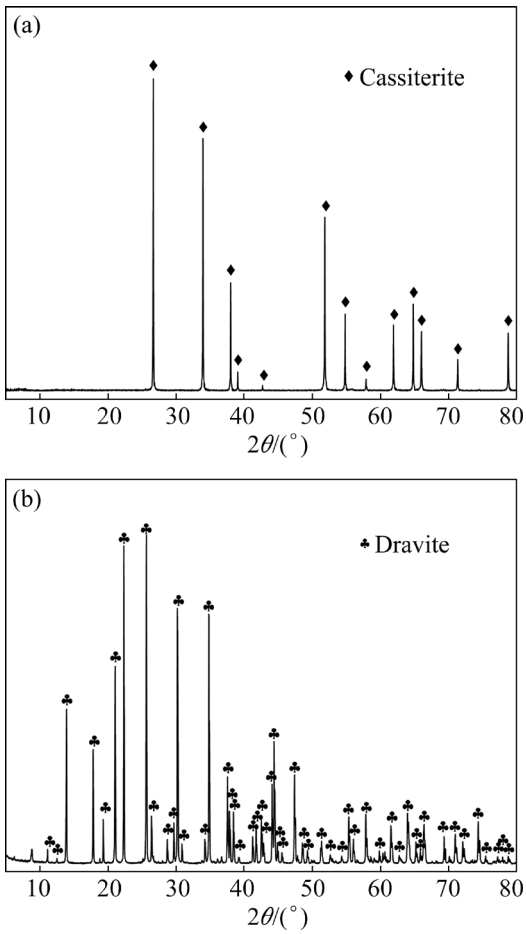

Fig. 1 XRD patterns of cassiterite (a) and dravite (b)

The reagents used in the experiments were all of analytical grade. Benzohydroxamic acid (BHA) was obtained from Shanghai Macklin Biochemical Co., Ltd., China. Lead nitrate ($Pb(NO_3)_2$) and terpilenol were purchased from Xilong Chemical Co., Ltd., Guangzhou, China. Sodium fluosilicate (Na_2SiF_6) was procured from Sinopharm Chemical Reagent Co., Ltd., Shanghai, China. Sodium hydroxide (NaOH) was purchased from Tianjin Hengxing Chemical Reagent Manufacturing Co., Ltd., China.

2.2 Micro-flotation experiments

The micro-flotation experiments were carried out in a flotation machine of XFG-type (Changchun Prospecting Machinery Factory, Jilin Province, China). The specific flowsheet is shown in Fig. 2. In each experiment, 2 g of single mineral and 35 mL of deionized water were mixed in a 40 mL flotation cell. Firstly, the flotation machine was operated at a constant impeller speed of 2000 r/min for 3 min. Subsequently, the depressant, collector,

and pH regulator were added sequentially, with each being stirred for 3 min. Finally, 1 μL of the frother (terpilenol) was added and the pulp was stirred for 1 min. Afterward, the froth products and tailings were collected, filtered, dried, and weighed, respectively. The recovery of micro-flotation was calculated by Eq. (1). Each experiment was conducted three times, and the final data were the average of the three replicates.

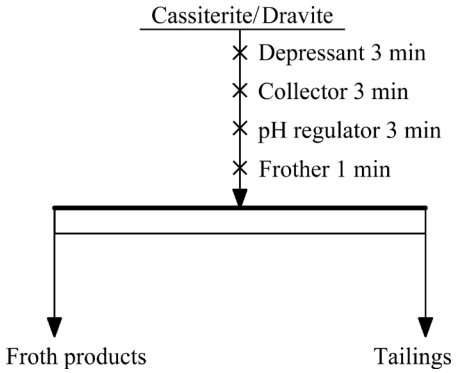

Fig. 2 Flowsheet of micro-flotation experiments

$$R=\frac{m_1}{m_1+m_2}\times 100\% \quad (1)$$

where R is the recovery of micro-flotation, m_1 (g) is the mass of the froth products, and m_2 (g) is the mass of the tailings.

2.3 Zeta potential tests

The zeta potentials of minerals treated and untreated with flotation reagents were measured using a JS94H microelectrophoresis instrument (Shanghai Zhongchen Digital Technology Instrument Co., Ltd., China) at 25 °C. Mineral samples weighing 0.04 g were placed in a 100 mL beaker. Subsequently, 70 mL of 10 mmol/L KCl solution was added as the supporting electrolyte. All samples were measured and recorded for at least three zeta potential values. Finally, the average zeta potential values were calculated, and zeta potential plots were made.

2.4 Fourier transform infrared (FTIR) spectroscopy tests

An IRAffinity model FTIR spectrophotometer (Shimadzu Instrument Co., Ltd., Japan) was used to perform the FTIR spectroscopy tests at 25 °C. Transmission mode was chosen for tests, with a wavelength range of 400−4000 cm^{-1}. 5 mg of mineral particles were mixed with 500 mg of dried potassium bromide and then manually ground using an agate mortar. The ground mixtures were then pressed into uniform thin wafers using a tablet press for subsequent tests.

2.5 X-ray photoelectron spectroscopy (XPS) tests

The XPS tests were performed using an ESCALAB Xi+ model XPS spectrometer (Thermo Fisher Scientific, USA). The samples were analyzed at 25 °C, with a measurement range of 0−1350 eV. The test results were fitted and calculated using Avantage analysis software.

3 Results and discussion

3.1 Micro-flotation results

Previous studies demonstrated that lead complexes of benzohydroxamic acid (Pb-BHA) can significantly enhance the flotation recovery of wolframite and cassiterite [23,24]. Accordingly, Pb-BHA was utilized in the micro-flotation experiments, with a fixed molar ratio of BHA to Pb^{2+} at 1:2 [19]. Additionally, the dosage of Pb-BHA was expressed as the concentration of BHA. In order to determine the optimum pH for flotation, pH experiments were carried out. As shown in Fig. 3, the recoveries of both dravite and cassiterite gradually increased with the elevation of flotation pH from 5.3 to 8.0. The recovery of cassiterite increased from 9.60% to 50.33%, and the recovery of dravite increased from 37.53% to 90.63%. Consequently, in the Pb-BHA system within the pH range of 5.3−8.0, the floatability of dravite is better than that of cassiterite. At pH 9.0, the recoveries of

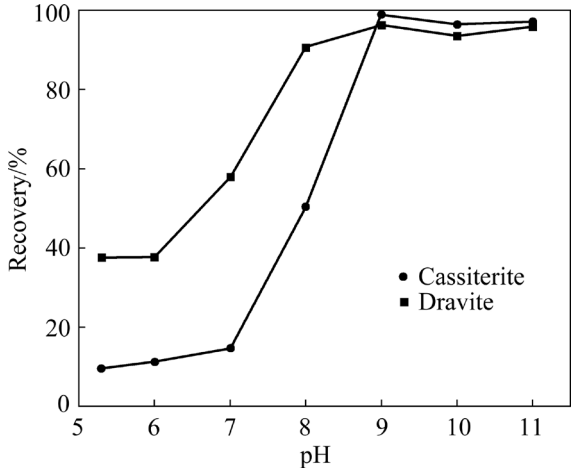

Fig. 3 Effect of pH on flotation of dravite and cassiterite at Pb-BHA dosage of 1.5×10^{-4} mol/L

both cassiterite and dravite were maximized at 98.57% and 96.13%, respectively. As the pH increased from 9.0 to 11.0, the recoveries of both dravite and cassiterite remained above 90%. Therefore, pH 9.0 was adopted for subsequent experiments. In addition, the results indicated that the recoveries of dravite and cassiterite in the Pb-BHA system showed no significant differences. Consequently, it is difficult to achieve effective separation of two minerals by merely adjusting the pH of flotation.

Figure 4 illustrates the effect of Pb-BHA dosage on the recoveries of dravite and cassiterite. With the elevation of Pb-BHA dosage, the recoveries of both dravite and cassiterite increased gradually. The recovery of cassiterite increased from 5.48% to 97.01%, and that of dravite increased from 58.01% to 95.88%, with the enhancement of collector dosage from 2.5×10^{-5} to 1.5×10^{-4} mol/L. Consequently, the collector dosage was determined as 1.5×10^{-4} mol/L. In addition, the results showed that dravite and cassiterite exhibited similar flotation behaviors in the Pb-BHA system. Consequently, effective flotation separation of cassiterite from dravite is hard without the addition of depressants.

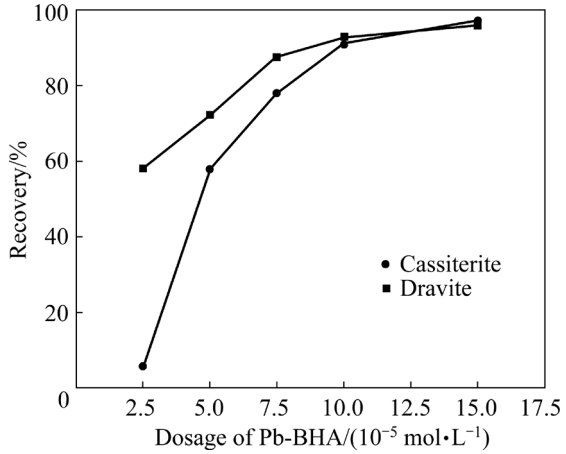

Fig. 4 Effect of Pb-BHA dosage on flotation of dravite and cassiterite at pH 9±0.1

As shown in Fig. 5, the recoveries of both cassiterite and dravite showed a declining trend with the enhancement of sodium fluosilicate (SF) dosage from 0 to 40 mg/L. As the dosage of SF increased from 0 to 15 mg/L, the recovery of cassiterite remained above 95%. Meanwhile, the recovery of dravite dropped abruptly from 95.88% to 25.14%. When the dosage of SF exceeded 15 mg/L, the recovery of dravite further decreased from 25.14% to less than 5%. Under identical conditions, the recovery of cassiterite also showed an obvious decline, from 96.61% to 3.26%. With the comprehensive comparison, the recovery difference between cassiterite and dravite was the largest at the depressant dosage of 15 mg/L, reaching 71.47%. Under these conditions, the flotation separation of dravite and cassiterite was optimal. Consequently, the flotation separation of cassiterite from dravite can be achieved by the addition of SF.

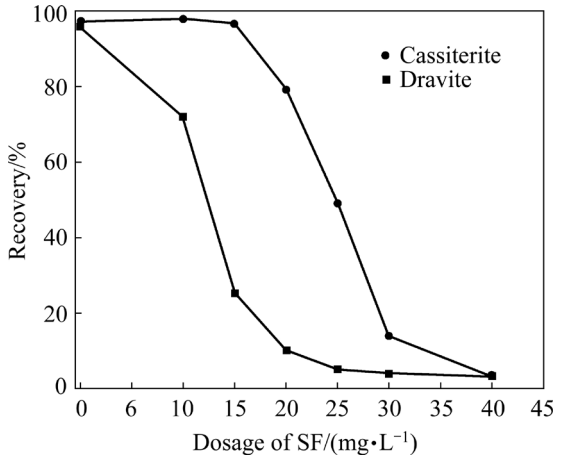

Fig. 5 Effect of SF dosage on flotation of dravite and cassiterite at Pb-BHA dosage of 1.5×10^{-4} mol/L and pH 9±0.1

3.2 Zeta potential results

Zeta potential tests were carried out to investigate the mechanism of flotation separation of cassiterite and dravite. Figures 6 and 7 show the curves of zeta potential variation of cassiterite and dravite as functions of pH under different conditions, respectively. The zeta potentials of untreated dravite and cassiterite were both negative within the pH range of 7.0−9.0. The zeta potential of dravite exhibited a positive shift of 35−55 mV upon the exclusive addition of Pb-BHA, whereas cassiterite showed a positive shift of 50−75 mV. It was demonstrated that significant adsorption of Pb-BHA occurred on the surfaces of both dravite and cassiterite. The more pronounced zeta potential shift of cassiterite indicated stronger adsorption of Pb-BHA, which was consistent with the flotation results (Fig. 3). At the SF dosage of 15 mg/L, the zeta potential of dravite exhibited a mean negative shift of approximately 5 mV. In contrast, the zeta potential of cassiterite demonstrated a mean

positive shift of about 10 mV. Notably, previous studies showed that the primary negatively charged components of sodium fluoro- silicate solutions are F^-, $SiO(OH)_3^-$, $SiO_2(OH)_2^{2-}$, and SiF_6^{2-} within the pH range of 7.0−9.0 [25−28]. Therefore, it could be concluded that SF could selectively adsorb onto the surface of dravite, leading to its selective depression.

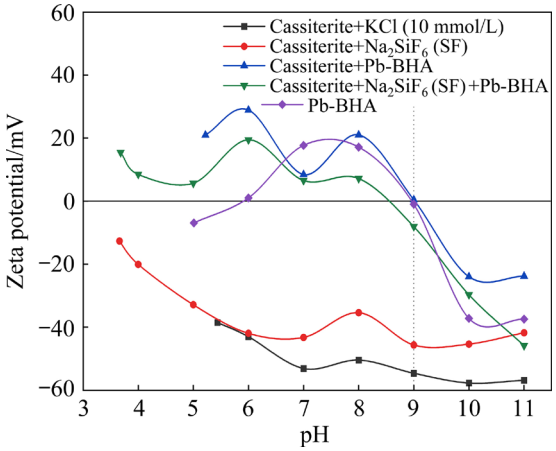

Fig. 6 Zeta potential of cassiterite as function of pH before and after treatment with reagents

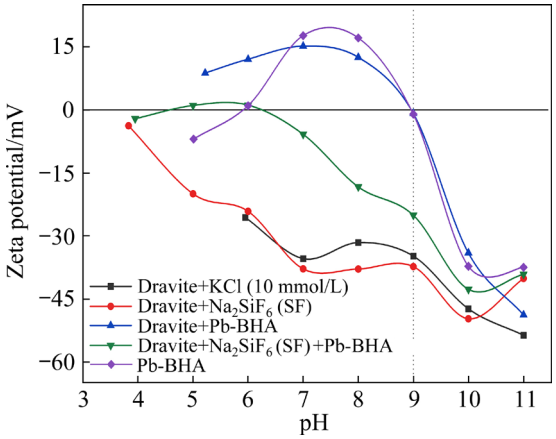

Fig. 7 Zeta potential of dravite as function of pH before and after treatment with reagents

Within the pH range of 7.0−9.0, the addition of Pb-BHA alone resulted in a positive zeta potential shift of 35−55 mV on the surface of dravite. In contrast, the sequential addition of SF followed by Pb-BHA reduced the positive shift to 9−30 mV. Meanwhile, within the pH range of 7.0−9.0, the zeta potential shift of cassiterite showed a positive shift of 50−75 mV, whether Pb-BHA was added alone or SF was added sequentially followed by Pb-BHA. In particular, the zeta potential of dravite showed a positive shift of 9.7 mV at pH 9.0, which was notably lower than the substantial 52.3 mV observed from cassiterite. The results demonstrated that the adsorption of SF on the dravite surface hindered the interaction between Pb-BHA and dravite, confirming the selective depression effect of SF on dravite, and providing further support for the flotation results (Fig. 5).

3.3 FTIR spectra

FTIR spectroscopy tests were conducted to elucidate the adsorption mechanism of flotation reagents (Pb-BHA, SF) on the surfaces of cassiterite and dravite. The results are presented in Figs. 8 and 9.

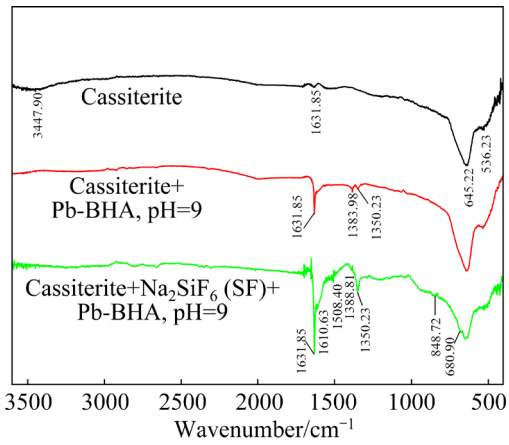

Fig. 8 FTIR spectra of cassiterite before and after treatment with reagents

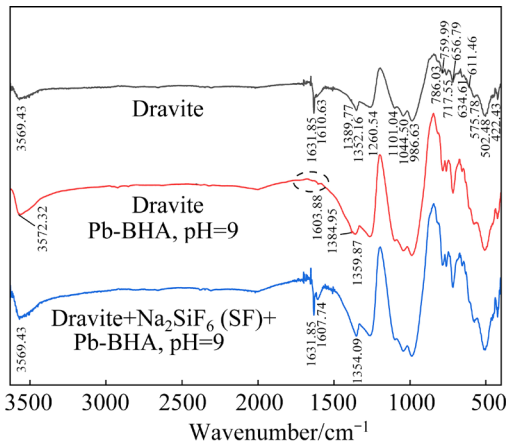

Fig. 9 FTIR spectra of dravite before and after treatment with reagents

In Fig. 8, the characteristic peaks at 645.22 and 536.23 cm^{-1} were generated by the asymmetric stretching vibration of the Sn—O bond and the symmetric stretching vibration of the O—Sn—O bond, respectively [16]. After the addition of Pb-BHA, three obvious new peaks at 1631.85,

1383.98 and 1350.23 cm^{-1} were found. These absorption peaks were attributed to functional groups of Pb-BHA [29]. This result indicated that the adsorption of Pb-BHA occurred on the surface of cassiterite. Furthermore, after the introduction of SF, the characteristic peaks of Pb-BHA did not disappear. On the contrary, some new characteristic peaks of Pb-BHA emerged in the spectrum. These results suggest that the addition of a certain amount of SF cannot generate efficient adsorption on cassiterite. The adsorption of Pb-BHA will not be hindered.

As shown in Fig. 9, the characteristic peaks of dravite were mainly in the interval of 1600−400 cm^{-1} [30]. The absorption peaks near 1630 and 3570 cm^{-1} were caused by hydroxyl groups and adsorbed water in dravite, respectively. The three absorption peaks in the interval of 1400−1200 cm^{-1} were attributed to the vibration of —BO_3 groups. The absorption peaks in the interval of 1200−900 cm^{-1} were attributed to the strong stretching vibration of Si—O. The absorption peaks in the interval of 800−600 cm^{-1} were derived from the vibration of B — O groups. Meanwhile, the absorption peaks in the interval of 750−550 cm^{-1} were associated with the symmetric stretching vibration of Si—O—Si, and the absorption peaks below 550 cm^{-1} were attributed to the vibration of Si—O, Al—O, and Mg—O. The absorption peaks at 1631.85 and 1610.63 cm^{-1} disappeared after the addition of Pb-BHA. It was attributed to the adsorption of Pb-BHA, which masked the vibrations of hydroxyl groups in dravite. On this basis, the two absorption peaks at 1631.85 and 1610.63 cm^{-1} did not disappear upon the addition of SF. It was attributed to the interaction between the hydroxyl-containing components, such as $SiO(OH)_3^-$ and $SiO_2(OH)_2^{2-}$, in the hydrolysis products of SF, and the active sites on the surface of dravite. Meanwhile, these hydroxyl-containing groups blocked the adsorption of Pb-BHA on dravite.

3.4 XPS spectra

XPS has been widely used in mineral engineering due to its excellent ability of qualitative, semi-quantitative analysis and structural identification of mineral surfaces [31]. Meanwhile, XPS can be used to identify the chemical bonding states of elements based on the chemical shifts resulting from changes in binding energy [32,33].

The flotation results showed that SF effectively adsorbed on the active sites of dravite, thereby reducing the adsorption of Pb-BHA. In contrast, SF exhibited a weak depression effect on cassiterite. As a result, the floatability difference between cassiterite and dravite was enlarged, enabling the flotation separation of cassiterite and dravite. The selective depression mechanism of SF was further analyzed by XPS. The results are shown in Figs. 10−12.

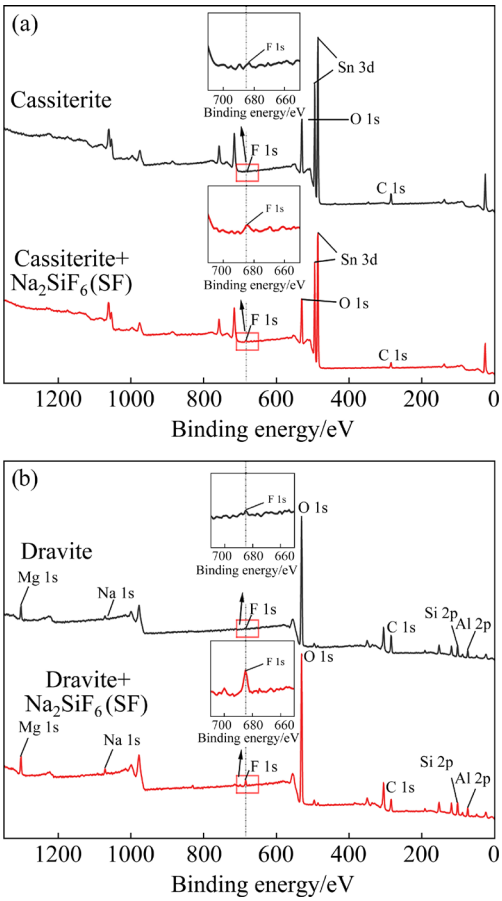

Fig. 10 XPS survey spectra of cassiterite (a) and dravite (b) before and after treatment with SF

Figure 10 illustrates the XPS survey spectra of cassiterite and dravite before and after the treatment with SF. As shown in Fig. 10(a), after the treatment with SF, a weak F 1s characteristic peak was found in the cassiterite spectrum, indicating that a small number of fluorine-containing components were adsorbed on its surface. In contrast, as shown in Fig. 10(b), a significant F 1s characteristic peak was found in the dravite spectrum, indicating that a significant number of fluorine-containing components were adsorbed on the surface of dravite. Therefore, the adsorption of SF on the dravite

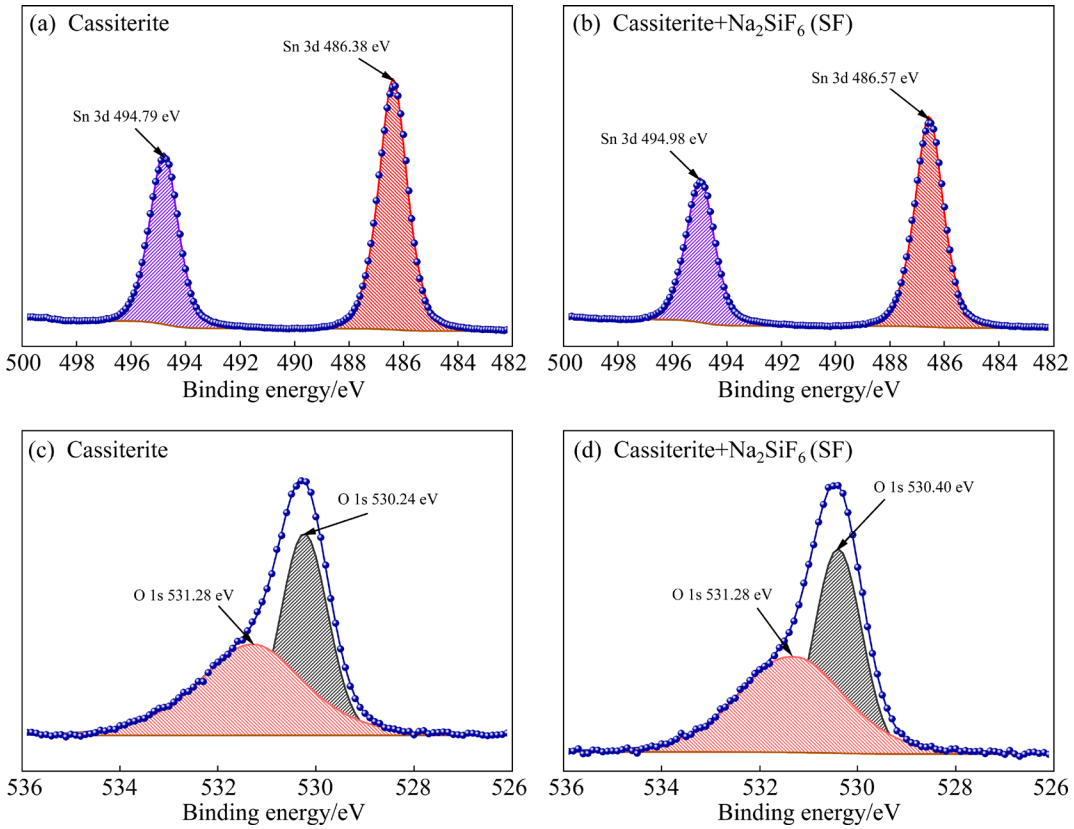

Fig. 11 Sn 3d XPS spectra of untreated (a) and SF-treated (b) cassiterite surface; O 1s XPS spectra of untreated (c) and SF-treated (d) cassiterite surface

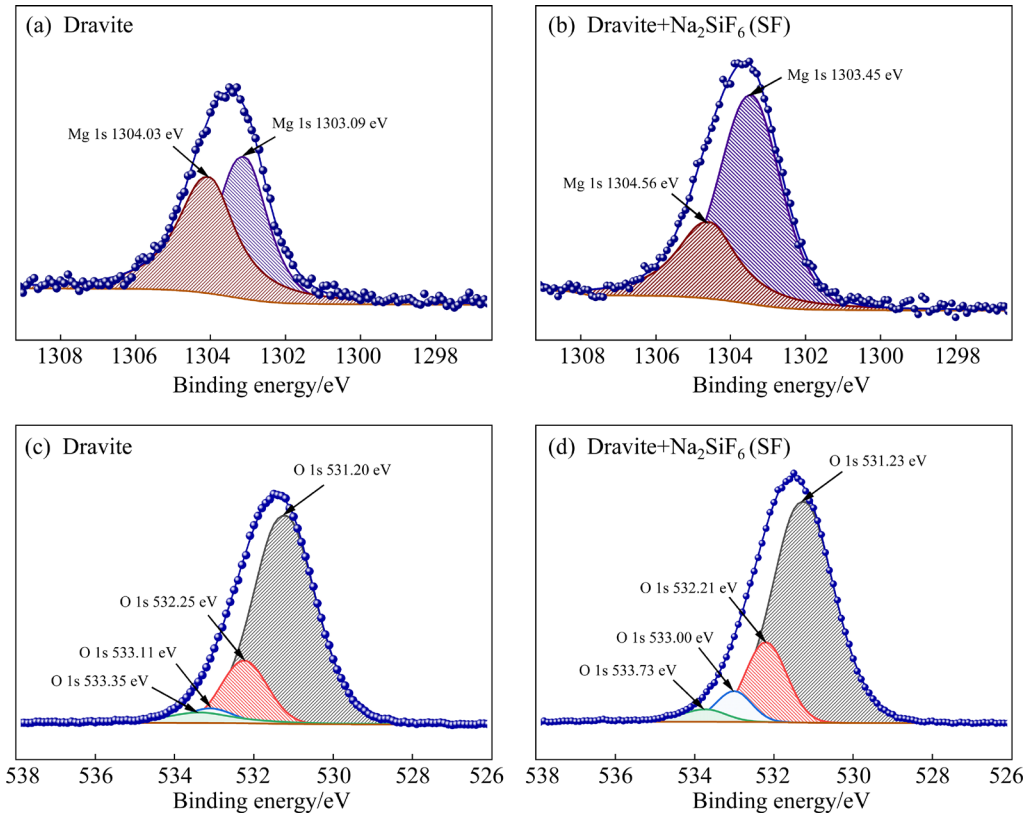

Fig. 12 Mg 1s XPS spectra of untreated (a) and SF-treated (b) dravite surface; O 1s XPS spectra of untreated (c) and SF-treated (d) dravite surface

surface is significantly stronger than that on the cassiterite surface.

Figure 11 shows the high-resolution XPS spectra of Sn 3d and O 1s on the cassiterite surface before and after treatment with SF. The observed peaks were similar to those reported for cassiterite in previous literature, with a deviation of ±0.2 eV [34,35]. The O 1s spectrum of untreated cassiterite exhibited two distinct peaks with binding energies of 530.24 and 531.28 eV. The peak at the binding energy of 530.24 eV belonged to the lattice oxygen atoms in the cassiterite, and the peak at the binding energy of 531.28 eV belonged to the oxygen atoms hydroxylated by Sn atoms on the surface of the cassiterite [36]. After the treatment with SF, the binding energy shifts of the energy levels of Sn $3d_{5/2}$ and Sn $3d_{3/2}$ were both 0.19 eV, and the binding energy shift of the O 1s peak (lattice oxygen atoms) at 530.24 eV was 0.16 eV. The binding energy shifts were within the error range. The results indicated that Sn and O atoms in cassiterite only weakly interacted with hydrolysis products of SF, indicating physisorption.

Figure 12 shows the XPS spectra of Mg 1s and O 1s on the dravite surface before and after treatment with SF. For the untreated dravite (Fig. 12(a)), the state of Mg 1s could be deconvoluted into two peaks at 1303.09 and 1304.03 eV, respectively. After the treatment with SF (Fig. 12(b)), the binding energy shifts of Mg 1s were 0.36 eV and 0.53 eV, respectively. These results showed that SF mainly interacted with Mg sites, leading to strong chemisorption on the surface of dravite. Meanwhile, four peaks were observed in Fig. 12(c). The peak at 533.73 eV was attributed to the oxygen atoms adsorbed on the dravite surface. These oxygen atoms resulted from the adsorption and hydrolysis of water molecules on the dravite surface [33,37−39]. This peak underwent a significant shift, proving that new hydroxyl-containing products appeared on the surface of dravite. In conjunction with the above results and Fig. 10, it could be deduced that the hydrolysis products of SF (F^-, $SiO(OH)_3^-$, $SiO_2(OH)_2^{2-}$, and SiF_6^-) reacted with Mg sites on the surface of dravite by chemisorption. This interaction resulted in the formation of F-containing hydrophilic products (MgF_2 and $MgSiF_6$) and hydroxyl-containing hydrophilic products ($(Mg(SiO(OH)_3)_2$ and $MgSiO_2(OH)_2$). The presence of these hydrophilic products prevented the adsorption of Pb-BHA on the surface of dravite and enhanced the wettability of dravite. Furthermore, Table 1 displays the binding energy shifts of Na 1s, Si 2p, Al 2p, and B 1s on the surface of dravite after treatment with SF, which are 0.18, 0.13, 0.12, and 0.09 eV, respectively. Therefore, SF adsorbed onto the surface of dravite by weak physisorption in addition to chemisorption.

Table 1 Binding energy shifts (Δ) of Na 1s, Si 2p, Al 2p, and B 1s on surface of dravite before and after treatment with SF

Element	Binging energy/eV		
	Before	After	Δ
Na 1s	1071.98	1072.16	0.18
Si 2p	102.22	102.35	0.13
Al 2p	74.39	74.51	0.12
B 1s	191.86	191.95	0.09

3.5 Selective depression model of SF

On the basis of the above analysis, a selective depression model of SF was constructed to explain the flotation separation of cassiterite and dravite, as shown in Fig. 13. The hydrolysis of SF generates the negatively charged groups such as F^-, $SiO(OH)_3^-$, $SiO(OH)_2^{2-}$ and SiF_6^{2-}. Under certain conditions, these components react with Mg sites on the surface of dravite by chemisorption, leading to the generation of F-containing hydrophilic products (MgF_2 and $MgSiF_6$) and hydroxyl-containing hydrophilic products ($(Mg(SiO(OH)_3)_2$ and $MgSiO_2(OH)_2$). Simultaneously, these hydrophilic components interact with other active sites of dravite (Al and Na sites) and cassiterite (Sn and O sites) by weak physisorption. The combination of strong chemisorption and weak physisorption can depress

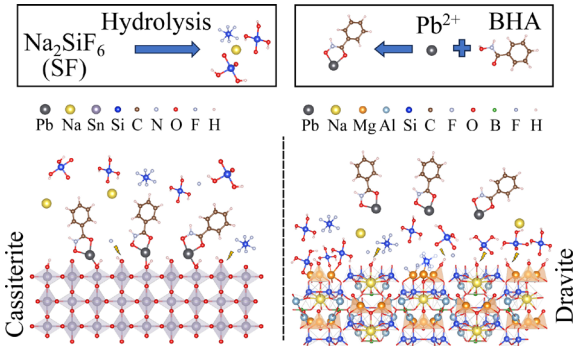

Fig. 13 Selective depression model of SF on cassiterite and dravite

effectively the collecting action of Pb-BHA on the surface of dravite. Nevertheless, the weak physisorption of SF cannot effectively prevent the collecting action of Pb-BHA on the surface of cassiterite. As a result, the selective depression of SF on dravite is realized.

4 Conclusions

(1) The effective flotation separation of dravite and cassiterite was achieved using sodium fluosilicate (SF) as a depressant and lead complexes of benzohydroxamic acid (Pb-BHA) as a collector.

(2) Micro-flotation results indicate that dravite and cassiterite have similar flotation performance under alkaline conditions (pH>8.0). Selective depression of dravite can be achieved by the addition of a specific amount of SF. The hydrolysis products of SF (F^-, SiF_6^{2-}, $SiO(OH)_3^-$ and $SiO_2(OH)_2^{2-}$) mainly interact with Mg sites of dravite by chemisorption, resulting in the formation of novel hydrophilic products. These hydrophilic products can effectively depress the adsorption of BHA on dravite and enhance the wettability of dravite. Inversely, the weak physisorption of SF cannot prevent the adsorption of Pb-BHA on the surface of cassiterite. Ultimately, the flotation separation of cassiterite and dravite can be achieved.

(3) The flotation separation of cassiterite and dravite has been studied in detail. However, there are still theoretical gaps regarding the surface properties of dravite. The development of reagent regimes for the flotation separation of cassiterite and dravite-associated gangue minerals is insufficient. Relevant theoretical researches still need to be continued.

CRediT authorship contribution statement

Yang NI: Data curation, Resources, Formal analysis, Investigation, Methodology, Visualization, Writing − Original draft preparation; **Wen-juan SUN:** Supervision, Investigation, Validation, Writing – Review & editing; **Hai-sheng HAN:** Supervision, Conceptualization, Formal analysis, Funding acquisition, Methodology, Project administration; **Wei SUN:** Supervision, Funding acquisition; **Jun-hao FU:** Investigation, Writing – Review & editing; **Yong-biao CHENG:** Supervision, Resources.

Declaration of competing interest

The authors declare that they have no known competing financial interests or personal relationships that could have appeared to influence the work reported in this paper.

Acknowledgments

This work was supported by the National Natural Science Foundation of China (No. 52122406), and the National Key Research Center and Development Program of the 14th Five-year Plan of China (Nos. 2022YFC2905104, 2022YFC2905105).

References

[1] CAO Yang, SUN Lei, WANG Qing-qing, WANG Xin, QIAO Yi, SUN Wei. DHX collector for recovery of cassiterite: Mechanistic insights and practical implications [J]. Journal of Industrial and Engineering Chemistry, 2023, 127: 210−217.

[2] ZHOU Wen-tao, HAN Yue-xin, SUN Yong-sheng, YANG Jin-lin, MA Shao-jian. Multi-scale impact crushing characteristics of polymetallic sulphide ores [J]. Transactions of Nonferrous Metals Society of China, 2019, 29(9): 1929−1938.

[3] WANG Xun, LIU Jie, ZHU Yi-min, LI Yan-jun. Selective adsorption of Na_2ATP as an eco-friendly depressant on the calcite surface for effective flotation separation of cassiterite from calcite [J]. Colloids and Surfaces A: Physicochemical and Engineering Aspects, 2021, 625: 126899.

[4] ZHANG Wei-di, LIU Shuang, REN Qi-long, TU Ru-yu, QIU Fen-hui, XU Shi-hong, SUN Wei, TIAN Meng-jie. Proposing a novel factor influencing flotation collector abilities to collect minerals by comparing two cationic collectors N,N-bis(2-hydroxy-3-chloropropyl) dodecylamine and dodecylamine [J]. Applied Surface Science, 2023, 640: 158284.

[5] ZHANG Wei-di, GUO Zhi-hao, LYU Fei, SUN Wei, GAO Zhi-yong, TIAN Meng-jie. Enhanced flotation separation of spodumene and albite via selective adsorption of N-hydroxy-9-octadecenamide on the mineral surfaces [J]. Minerals Engineering, 2023, 199: 108117.

[6] ZHAO Guan-fei, FENG Bo, ZHU Dong-mei, QIU Xian-hui, GAO Zhi-yong, YAN Hua-shan, LAI Rui-seng, QIU Ting-sheng. Enhanced separation of scheelite and calcite by metal-inorganic complex depressant [J]. Transactions of Nonferrous Metals Society of China, 2024, 34(2): 643−654.

[7] ZHANG Ga, WANG Mei-li, HE Yong-xin, WANG Han, FENG Qi-cheng. Sulfidization performance of hemimorphite surface in sodium sulfide system and identification of sulfidization products [J]. Transactions of Nonferrous Metals Society of China, 2024, 34(2): 629−642.

[8] PAN Zu-chao, ZHANG Yi-sheng, HU Jun-jie, JIAO Fen, QIN Wen-qing. Camphor leaf extract as neoteric and environmentally friendly depressant in flotation separation of scheelite and calcite [J]. Transactions of Nonferrous Metals Society of China, 2023, 33(1): 275−284.

[9] GONG Gui-chen, LIU Jie, HAN Yue-xin, ZHU Yi-min. Study on flotation performances and adsorption mechanism of 2-carboxyethylphenylphosphinic acid to cassiterite [J].

Separation Science and Technology, 2019, 54(11): 1815−1828.

[10] SUN Lei, HU Yue-hua, SUN Wei. Effect and mechanism of octanol in cassiterite flotation using benzohydroxamic acid as collector [J]. Transactions of Nonferrous Metals Society of China, 2016, 26(12): 3253−3257.

[11] HE Jian-yong, SUN Wei, CHEN Dai-xiong, GAO Zhi-yong, ZHANG Chen-yang. Interface interaction of benzohydroxamic acid with lead ions on oxide mineral surfaces: A coordination mechanism study [J]. Langmuir, 2021, 37(11): 3490−3499.

[12] OU Le-ming, YANG Hao. Comparing cyclohexyl hydroxamic acid and benzohydroxamic acid in cassiterite flotation under lead nitrate activation [J]. Physicochemical Problems of Mineral Processing, 2023, 59(6): 174673.

[13] CAO Yang, SUN Lei, GAO Zhi-yong, SUN Wei, CAO Xue-feng. Activation mechanism of zinc ions in cassiterite flotation with benzohydroxamic acid as a collector [J]. Minerals Engineering, 2020, 156: 106523.

[14] TIAN Meng-jie, GAO Zhi-yong, HAN Hai-sheng, SUN Wei, HU Yue-hua. Improved flotation separation of cassiterite from calcite using a mixture of lead (II) ion/benzo-hydroxamic acid as collector and carboxymethyl cellulose as depressant [J]. Minerals Engineering, 2017, 113: 68−70.

[15] WU X Q, ZHU J G. Selective flotation of cassiterite with benzohydroxamic acid [J]. Minerals Engineering, 2006, 19(14): 1410−1417.

[16] TIAN Meng-jie, GAO Zhi-yong, JI Bin, FAN Rui-ying, LIU Run-qing, CHEN Pan, SUN Wei, HU Yue-hua. Selective flotation of cassiterite from calcite with salicylhydroxamic acid collector and carboxymethyl cellulose depressant [J]. Minerals, 2018, 8(8): 316.

[17] NIE Si-yue, GUO Zhi-hao, TIAN Meng-jie, SUN Wei. Selective flotation separation of cassiterite and calcite through using cinnamohydroxamic acid as the collector and Pb^{2+} as the activator [J]. Colloids and Surfaces A: Physicochemical and Engineering Aspects, 2023, 666: 131262.

[18] LU Yu-xi, WANG Shuai, ZHONG Hong. Optimization of conventional hydroxamic acid for cassiterite flotation: Application of structural modification under principle of isomerism [J]. Minerals Engineering, 2021, 167: 106901.

[19] HAN Hai-sheng, LIU Wen-Li, HU Yue-hua, SUN Wei, LI Xiao-dong. A novel flotation scheme: Selective flotation of tungsten minerals from calcium minerals using Pb–BHA complexes in Shizhuyuan [J]. Rare Metals, 2017, 36(6): 533−540.

[20] HAN Hai-sheng, HU Yue-hua, SUN Wei, LI Xiao-dong, CAO Chong-gao, LIU Run-qing, YUE Tong, MENG Xiang-song, GUO Yan-zhe, WANG Jian-jun, GAO Zhi-yong, CHEN Pan, HUANG Wei-sheng, LIU Jie, XIE Jia-wen, CHEN Yu-lin. Fatty acid flotation versus BHA flotation of tungsten minerals and their performance in flotation practice [J]. International Journal of Mineral Processing, 2017, 159: 22−29.

[21] HOUCHIN M R. Surface studies on aqueous suspensions of tourmaline (dravite) [J]. Colloids and Surfaces, 1986, 19(1): 67−82.

[22] BOSI F. Tourmaline crystal chemistry [J]. American Mineralogist, 2018, 103(2): 298−306.

[23] WEI Zhao, SUN Wei, HAN Hai-sheng, XING Yao-wen, GUI Xia-hui. Molecular design of multiple ligand metal–organic framework (ML-MOF) collectors for efficient flotation separation of minerals [J]. Separation and Purification Technology, 2024, 328: 125048.

[24] WEI Zhao, SUN Wei, WANG Ping-shan, HAN Hai-sheng, LIU Die. The structure analysis of metal–organic complex collector: From single crystal, liquid phase, to solid/liquid interface [J]. Journal of Molecular Liquids, 2023, 382: 122029.

[25] BERGER G S, BULATOVA E V. Mechanism of the activating and depressing effects of sodium fluosilicate in the flotation of minerals by oleate soap [J]. Soviet Mining Science, 1969, 5(4): 452−456.

[26] CHEN Qian, TIAN Mao-mao, ZHENG Hui-fang, LUO Hui-hua, LI Hong-qiang, SONG Shao-xian, HE Dong-sheng, JIANG Xin-hua. Flotation of rutile from almandine using sodium fluorosilicate as the depressant [J]. Colloids and Surfaces A: Physicochemical and Engineering Aspects, 2020, 599: 124918.

[27] DONG Liu-yang, JIAO Fen, QIN Wen-qing, ZHU Hai-ling, JIA Wen-hao. Selective depressive effect of sodium fluorosilicate on calcite during scheelite flotation [J]. Minerals Engineering, 2019, 131: 262−271.

[28] WARREN L J. Flocculation of stirred suspensions of cassiterite and tourmaline [J]. Colloids and Surfaces, 1982, 5(4): 301−319.

[29] HE Jian-yong, HAN Hai-sheng, ZHANG Chen-yang, XU Zhi-jie, YUAN Dan-dan, CHEN Pan, SUN Wei, HU Yue-hua. Novel insights into the surface microstructures of lead (II) benzohydroxamic on oxide mineral [J]. Applied Surface Science, 2018, 458: 405−412.

[30] FAWZY M M. Flotation separation of dravite from phlogopite using a combination of anionic/nonionic surfactants [J]. Physicochemical Problems of Mineral Processing, 2021, 57(4): 87−95.

[31] ONYIRIUKA E C. Zinc phosphate glass surfaces studied by XPS [J]. Journal of Non-Crystalline Solids, 1993, 163(3): 268−273.

[32] MOFFAT T P, LATANISION R M, RUF R R. An X-ray photoelectron spectroscopy study of chromium-metalloid alloys−III [J]. Electrochimica Acta, 1995, 40(11): 1723−1734.

[33] JOYNER D J, HERCULES D M. Chemical bonding and electronic structure of B_2O_3, H_3BO_3, and BN: An ESCA, Auger, SIMS, and SXS study [J]. The Journal of Chemical Physics, 1980, 72(2): 1095−1108.

[34] FAN Hong-li, GAO Yue-sheng, SUN Wei, LI Jian-fei. Enhancing cassiterite flotation by 1-hydroxy-dodecyl-idene-1,1-diphosphonic acid (HDDPA) [J]. Minerals Engineering, 2024, 206: 108521.

[35] TIAN Meng-jie, HU Yue-hua, SUN Wei, LIU Run-qing. Study on the mechanism and application of a novel collector−complexes in cassiterite flotation [J]. Colloids and Surfaces A: Physicochemical and Engineering Aspects, 2017, 522: 635−641.

[36] MIAO Yong-chao, FENG Qi-cheng, WEN Shu-ming. Experimental and MD study on the effect of SDS/OHA mixed collector co-adsorption on cassiterite flotation [J].

Separation and Purification Technology, 2024, 339: 126635.
[37] IDRISS H. On the wrong assignment of the XPS O 1s signal at 531−532 eV attributed to oxygen vacancies in photo- and electro-catalysts for water splitting and other materials applications [J]. Surface Science, 2021, 712: 121894.
[38] WAGNER C D, PASSOJA D E, HILLERY H F, KINISKY T G, SIX H A, JANSEN W T, TAYLOR J A. Auger and photoelectron line energy relationships in aluminum–oxygen and silicon–oxygen compounds [J]. Journal of Vacuum Science and Technology, 1982, 21(4): 933−944.
[39] SEYAMA H, SOMA M. Bonding-state characterization of the constituent elements of silicate minerals by X-ray photoelectron spectroscopy [J]. Journal of the Chemical Society, 1985, 81(2): 485−495.

氟硅酸钠在锡石和镁电气石浮选分离中的选择性抑制作用

倪 扬[1]，孙文娟[1]，韩海生[1,2,3]，孙 伟[1,2]，付君浩[1]，程永彪[1]

1. 中南大学 资源加工与生物工程学院，长沙 410083；
2. 中南大学 金属资源开发利用碳减排教育部工程研究中心，长沙 410083；
3. 湖南省伴生萤石综合利用氟化学工程技术研究中心，郴州 423000

摘 要：以苯甲羟肟酸铅(Pb-BHA)配合物为捕收剂、氟硅酸钠(SF)为抑制剂，实现了锡石与镁电气石的浮选分离。Zeta 电位实验结果证实 SF 对镁电气石具有选择性抑制作用。傅里叶红外光谱(FTIR)分析结果表明，SF 水解产物中的含羟基基团可以实现对镁电气石表面的选择性化学吸附。X 射线光电子能谱(XPS)测试进一步证明 SF 水解产物(含 F 基团和含羟基基团)在镁电气石(Mg 位点)表面发生了强烈的化学吸附。因此，Pb-BHA 对镁电气石的吸附被选择性地阻止。在此基础上，提出了 SF 对镁电气石和锡石的选择性抑制模型。

关键词：选择性抑制作用；浮选分离；氟硅酸钠；锡石；镁电气石；苯甲羟肟酸

(Edited by Wei-ping CHEN)